Renewable Energy 60 (2013) 462–471

Contents lists available at SciVerse ScienceDirect

Renewable Energy

journal homepage: www.elsevier.com/locate/renene

Improving the assessment of wave energy resources by means of coupled wave-ocean numerical modeling

Francesco Barbariol [a], Alvise Benetazzo [b], Sandro Carniel [b], Mauro Sclavo [b,*]

[a] Department of Civil, Environmental, and Architectural Engineering (ICEA), University of Padua, Padua, Italy
[b] Institute of Marine Sciences-National Research Council (ISMAR-CNR), Venice, Italy

ARTICLE INFO

Article history:
Received 21 November 2012
Accepted 19 May 2013
Available online 15 June 2013

Keywords:
Wave power
Wave energy
Adriatic Sea
Gulf of Venice
Wave–Current Interaction (WCI)
ROMS–SWAN

ABSTRACT

Sea waves energy represents a renewable and sustainable energy resource, that nevertheless needs to be further investigated to make it more cost-effective and economically appealing. A key step in the process of Wave Energy Converters (WEC) deployment is the energy resource assessment at a sea site either measured or obtained through numerical model analysis. In these kind of studies, some approximations are often introduced, especially in the early stages of the process, viz. waves are assumed propagating in deep waters without underneath ocean currents. These aspects are discussed and evaluated in the Adriatic Sea and its northern part (Gulf of Venice) using locally observed and modeled wave data. In particular, to account for a "state of the art" treatment of the Wave–Current Interaction (WCI) we have implemented the Simulating WAves Nearshore (SWAN) model and the Regional Ocean Modeling System (ROMS), fully coupled within the Coupled Ocean Atmosphere Wave Sediment Transport (COAWST) system. COAWST has been applied to a computational grid covering the whole Adriatic Sea and off-line nested to a high-resolution grid in the Gulf of Venice. A 15-year long wave data set collected at the oceanographic tower "Acqua Alta", located approximately 15 km off the Venice coast, has also been analyzed with the dual purpose of providing a reference to the model estimates and to locally assess the wave energy resource. By using COAWST, we have quantified for the first time to our best knowledge the importance of the WCI effect on wave power estimation. This can vary up to 30% neglecting the current effect. Results also suggest the Gulf of Venice as a suitable testing site for WECs, since it is characterized by periods of calm (optimal for safe installation and maintenance) alternating with severe storms, whose wave energy potentials are comparable to those ordinarily encountered in the energy production sites.

1. Introduction

In a context of oil fields depletion and environmental care, community interest on renewable and sustainable energy resources is growing year by year. Marine energy, i.e. derived from wind, tides and waves, is considered as one of the most promising energy resources. Hence, many efforts are being globally invested in the research. The development of standards and protocols for the deployment of marine energy devices is one of the targets of the EU projects ORECCA (Off-shore Renewable Energy Conversion platforms – Coordination Action [1]), MARINA (Marine Renewable Integrated Application Platform [2]) and EquiMar (Equitable Testing and Evaluation of Marine Energy Extraction Devices in terms of Performance, Cost and Environmental Impact [3]).

Wind waves spanning the world seas represent a strategic power source, globally estimated to be 2.11 TW [4]. Indeed, several Wave Energy Converters (WEC) have been designed and tested [5] to make wave energy also an economically appealing resource. An accurate assessment of the potential energy that can be extracted from wind waves in a particular site of interest remains a crucial step in the deployment process of a "wave energy farm" [6,7]. Estimated wave energy potentials have been collected in atlases and databases. WorldWave Atlas [8] provides worldwide average wave power data while WERAtlas [9] covers the North-Eastern Atlantic Ocean, the North Sea, the Norwegian Sea, the Barents Sea and the Mediterranean Sea. However, the accuracy of the wave power characterization may be affected by several aspects, that have been recently remarked in the context of the EU project EquiMar [3]. Firstly, when assessments are based on wave time

* Corresponding author.
E-mail address: mauro.sclavo@ismar.cnr.it (M. Sclavo).

0960-1481/$ – see front matter © 2013 Elsevier Ltd. All rights reserved.
http://dx.doi.org/10.1016/j.renene.2013.05.043

series, measured or modeled, these should be long enough to be representative of the wave climate at the chosen sea site. A minimum duration of 10 years should be advisable, to catch the interannual variability of the resource. Secondly, wave power is a depth-dependent quantity, hence an accurate evaluation should consider the actual relative water depth (d/L, being d water depth and L wavelength). A deep waters approximation could be used only in the early stages of the deployment process, unless the WEC is indeed positioned in deep waters. Then, wave power fields obtained from numerical models should result from a complete modeling of the phenomena involved in the wave evolution and affecting it, e.g. accounting also for Wave–Current Interactions (WCI). EquiMar protocols recommend ocean currents modeling if their velocity is greater than 2–3% of the local group velocity of the dominant waves (e.g. for an 8 s period deep-waters wave, current must be taken into account if greater than 0.2 m/s). Finally, regarding model grid a spatial resolution of 1.0–5.0 km, increased in case of wave-current modeling (<0.5 km), is recommended. If bathymetry data availability and computational resources allow it, 0.2 km is the spatial resolution advised.

All these aspects are here discussed performing wave energy assessments from both high-resolution numerical modeling and wave measurements. The test field chosen is the northern Adriatic Sea (Fig. 1), where the average wave power was estimated in the order of 2–3 kW/m [10,11], less than other seas characterized by stronger wave climates, e.g. the eastern Atlantic Ocean (50 kW/m of average wave power), deeply investigated from Ireland down to Spain, since the 1980s [12]. On the contrary, the whole Mediterranean basin has been less studied until now with the needed accuracy. However, Mediterranean wave energy potentials can be easily obtained by consulting the ORECCA WebGIS (map.rse-web.it/orecca/map.phtml), collecting WorldWave Atlas and WERAtlas databases in the Mediterranean Sea. The average wave power there can exceed 10 kW/m, as other authors showed [11,13].

We have assessed the energy resource in the northern Adriatic Sea, in particular in the Gulf of Venice, using numerical data computed coupling the Simulating WAves Nearshore model (SWAN [14]) and the Regional Ocean Modeling System (ROMS [15]) on the same computational grid, within the COAWST modeling system [16,17]. A 1-year long simulation (September, 2010–August, 2011) has been run on the whole Adriatic Sea, with a 2.0 km spatial resolution, and nested in the Gulf of Venice to a 0.5 km computational grid over the winter season (January–March, 2011). We have performed coupled (waves and currents) and uncoupled (only waves) COAWST runs, to quantify for the first time the WCI effect on wave power estimation. Recently some authors [18–21] have highlighted the relevance of using high spatial resolution wind inputs to correctly reproduce the circulation patterns in the Adriatic Sea, especially those generated by Bora wind. Following these suggestions the atmospheric forcing was provided by the high-resolution (7.0 km) COSMO-I7 model [22]. This aspect was also stressed to be fundamental in order to estimate the wave energy distribution in the Adriatic Sea [11], and filling this gap is one of the purposes of the present work.

We also characterized the northern Adriatic Sea wave energy potential using 15 years (1996–2011) of wave observations, gathered at ISMAR-CNR oceanographic tower "Acqua Alta" (Fig. 1). Besides the purpose of a long-term evaluation from measured data, we have used this data set as the benchmark for comparing the numerical model estimate and check the improvement obtained in wave energy assessment by including WCI modeling. "Acqua Alta" tower data set has been also used to investigate the effect of using a depth-dependent wave power formulation rather than a deep-waters formula.

The paper is structured as follows. Section 2 describes theoretical, numerical and experimental tools used for the wave power assessments. Section 3 contains the energy resource characterization over the northern Adriatic Sea through numerical modeling and oceanographic tower "Acqua Alta" wave data set. Discussions on the improvements of energy resource assessment are herein included. Final considerations, in Section 4, complete the paper.

2. Theoretical, numerical and experimental tools

2.1. Wave power calculation

In random seas, the flux of wave energy, i.e. the wave power $\boldsymbol{P}$, is a vector quantity defined as [12]:

$$\boldsymbol{P} = \int\int \boldsymbol{c_g}(\sigma,d)E(\sigma,\theta)\mathrm{d}\sigma\mathrm{d}\theta = \rho g \int\int \boldsymbol{c_g}(\sigma,d)S(\sigma,\theta)\mathrm{d}\sigma\mathrm{d}\theta \tag{1}$$

where σ, θ, and d are the intrinsic wave frequency, direction of wave propagation and water depth respectively, and $\boldsymbol{c_g}(\sigma, d)$ is the wave group celerity vector. In Eq. (1)ρ is the water density in kg/m^3, and g is the gravitational acceleration. $E(\sigma, \theta)$ and $S(\sigma, \theta)$, the energy and variance directional spectra respectively, can be provided by directional wave measurements or numerical spectral wave models. Alternatively to Eq. (1), equations based on bulk spectral parameters, i.e. significant wave height H_{m0} (m), and mean wave period T_m (s), can be used to estimate $\boldsymbol{P}$. To this end, Eq. (1) is rewritten assuming a constant group celerity, corresponding to the spectral average frequency σ_m:

$$\boldsymbol{P} \simeq \boldsymbol{c_g}(\sigma_m, d)\rho g \int\int S(\sigma,\theta)\mathrm{d}\sigma\mathrm{d}\theta = \boldsymbol{c_g}(\sigma_m, d)\overline{E} = \boldsymbol{c}_{\boldsymbol{g},\mathrm{m}}\overline{E} \tag{2}$$

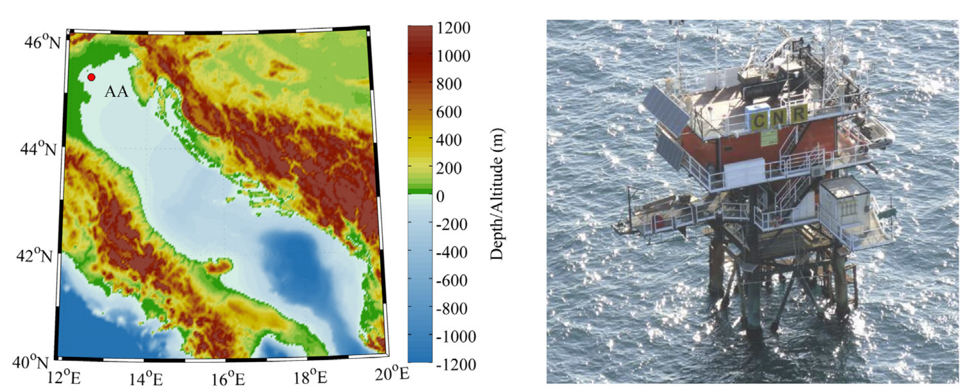

Fig. 1. Left: Adriatic Sea bathymetry and surrounding orography. Right: ISMAR-CNR oceanographic tower "Acqua Alta" (AA, in left panel).

In Eq (2), $\overline{E}$ is the specific wave energy, that can be expressed in terms of H_{m0} as $\overline{E} = \rho g H_{m0}^2/16$ (kJ/m^2). Switching to vectors norm, the following well known equation of wave power per unit crest length P (kW/m) is obtained:

$$P \simeq c_{g,m}\overline{E} = c_{g,m}\frac{\rho g}{16}H_{m0}^2 \tag{3}$$

The group celerity (m/s) can be expressed as:

$$c_{g,m} = \frac{1}{2}\left(1+\frac{2k_m d}{\sinh 2k_m d}\right)\sqrt{\frac{g}{k_m}\tanh k_m d} \tag{4}$$

where k_m is the modulus of the average wavenumber vector, implicitly defined within the linear dispersion relation: $\sigma_m^2 = (2\pi/T_m)^2 = gk_m \tanh k_m d$.

The total wave energy E_{tot} (kW h/m or MW h/m), potentially produced during a given time interval $T = \sum_i \delta t_i$ (expressed in hours h; $i = 1, 2, \ldots n$), is given by:

$$E_{tot} = \sum_i P_i \delta t_i \tag{5}$$

The mean wave period used for wave energy assessments is the so called "energy period" T_e[23]:

$$T_e = T_{m-10} = 2\pi\frac{m_{-1}}{m_0} \tag{6}$$

where $m_i = \int\int \sigma^i S(\sigma,\theta)\mathrm{d}\sigma\mathrm{d}\theta$ is the i-th moment of $S(\sigma,\theta)$ [24]. Eqs. (3) through (6) allow to estimate P from bulk wave data and accounting for the water depth d. A simplified formula strictly valid in deep waters ($d/L \to \infty$, being L the wavelength) is often used (see for example [25]):

$$P_{dw} = \frac{\rho g^2}{64\pi}H_{m0}^2 T_e \tag{7}$$

We notice that the above Equation is routinely used for wave power estimation, even when the deep waters hypothesis is not strictly satisfied.

2.2. Observations and modeling of Adriatic Sea states

The Adriatic Sea (Fig. 1, left) is an elongated (approximately 700 km long and 200 km wide) semi-enclosed basin located in the north-eastern part of the Mediterranean Sea. It is surrounded by the Italian peninsula and Balkan regions and connected to the Mediterranean Sea through Otranto Strait. The northern part of Adriatic Sea (Gulf of Venice) has relatively shallow waters and mild bottom slopes, while the southern part of it reaches the maximum water depths, up to −1200 m a.m.s.l. The most frequent winds blowing over the Adriatic Sea are Bora and Sirocco, both responsible for high waves generation over the basin during storm events. In the Gulf of Venice, waves up to 3.5 m of significant wave height have been observed in several occasions [18,26]. Bora is a fetch-limited, dry and cold wind, blowing from North-East. During winter Bora blows particularly strong over the northern and central Adriatic Sea (up to 15 m/s for several days, with gusts up to 50 m/s), causing enhanced local cyclonic oceanic flow [27,28]. Sirocco is a wet wind, blowing from south-eastern quadrant. It is not fetch-limited and it grows slowly, reaching highest speeds on the eastern regions and decreasing while proceeding towards the western coasts [18]. In the semi-enclosed Adriatic Sea, especially in its northern part, ocean currents are mainly generated and driven by wind. In the Gulf of Venice they are 0.2 m/s on average, though local 0.8 m/s current were measured by Book et al. [29].

An analysis aimed at quantifying the energy resource in the northern Adriatic Sea was performed by Vicinanza et al. [10], based on an 11-month data set collected at "Punta della Maestra" buoy (Lat = 44° 58′ 18″ N, Lon = 12° 49′ 59″ E), deployed at 30 m water depth. In the present paper, we have extended this assessment using longer observational data consisting in a 15-year long wave time series acquired at the ISMAR-CNR oceanographic tower "Acqua Alta" (Lat = 45° 18′ 83″ N, Lon = 12° 30′ 53″ E, Fig. 1), located approximately 15 km off the Venice coast and 45 km far from Punta della Maestra buoy, at 16 m water depth. Significant wave height H_{m0} and mean wave period T_{m01} (Fig. 2) were measured from August 1st, 1996 to July 31st, 2011 (referred hereinafter as 1996–2011). As stated by other studies (e.g. Ref. [3]), the 15-year long time series is extended enough to describe the wave climate at the "Acqua Alta" site and in the northern Adriatic Sea as well, and allows to consider the long term climatological variations of a higher order.

Adriatic Sea and Gulf of Venice sea waves and currents have been herein modeled using the Coupled Ocean-Atmosphere-Wave-Sediment Transport (COAWST) modeling system [30], namely coupling the wave model SWAN (Simulating WAves Nearshore, see Ref. [14] and www.swan.tudelft.nl) and the ocean model ROMS (Regional Ocean Modeling System [15]). The coupling has been synchronous with ROMS providing to SWAN the following fields: free surface elevation, bathymetry, and 2-D current (the horizontal components of the 3-D current velocity field have been transformed using the formulation proposed by Kirby and Chen [31] which accounts for the wavelength to average the non-uniform

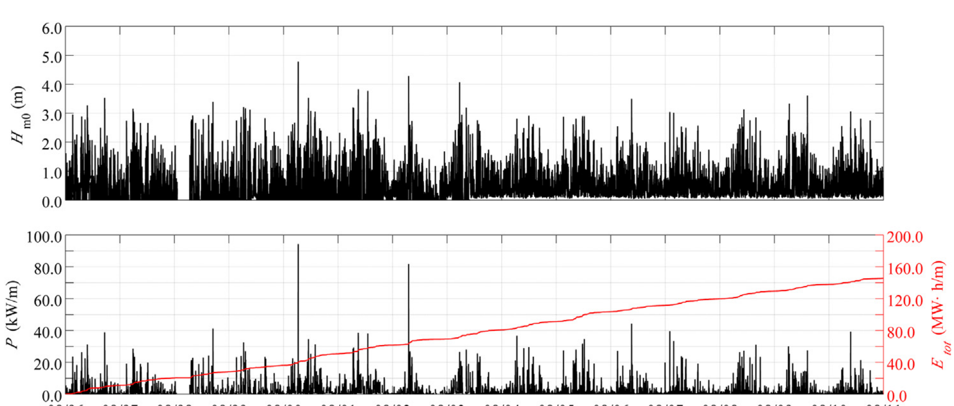

Fig. 2. Time series of observed significant wave height H_{m0} (top panel) and wave power (bottom panel) P at the oceanographic tower "Acqua Alta" (1996–2011). On the bottom panel the total potentially produced energy E_{tot} is drawn in red. (For interpretation of the references to color in this figure legend, the reader is referred to the web version of this article.)

vertical current profile). Within SWAN, ocean circulation modulates the wave action density transport, generates a current-induced refraction, and also modifies the local wind stress on the water surface. In COAWST, wave effects on the oceanic circulation have been accounted for by using a Vortex Force (VF) formalism [32]. Differently than in the radiation stress approach [33], VF decomposes advection terms in the equations of motion by means of the Helmholtz decomposition [34]. VF considers wave effects averaged in a Eulerian reference frame, entering in ROMS primitive equations as momentum and tracers fluxes. VF separates hydrodynamic contributions in conservative and non-conservative (i.e. dissipative) wave forces, adjusting the pressure field to satisfy the presence of surface waves.

SWAN has been run in third generation mode, assuming an exponential wave growth [35], whitecapping dissipation term, and the Discrete Interaction Approximation [36] to simulate the quadruplet wave–wave interactions in deep waters. Dissipation terms due to bottom friction and depth-induced wave breaking have been also accounted for. SWAN has been run discretizing the wave action density with 24 equally spaced directions and 32 intrinsic frequencies f, between the lowest (0.05 Hz) and the highest (1.00 Hz) discrete frequencies. Computed significant wave height (H_{m0}), wave period ($T_{m-10} = T_e$), and mean wave direction (θ) has been saved with a 3-h time step.

In the Adriatic Sea, COAWST has been implemented on two different computational grids: a parent coarse (C) grid (with horizontal resolution of 2.0 km) covering the whole Adriatic Sea, and a child fine (F) grid covering the Gulf of Venice at a resolution of 0.5 km (Table 1). On the parent grid, waves and currents have been simulated for a 1-year period bracketing September, 2010–August, 2011, whereas the child grid has been 1-way nested to the parent grid for the winter period January–March, 2011. The Mediterranean Forecasting System [37] (through MyOcean, www.myocean.eu.org) provided the southern open boundary conditions for ROMS, in terms of sea surface elevation, vertical distribution of 2-D momentum, temperature and salinity. On the same boundary, five tidal constituents (M2, S2, N2, 01, K1) from the Oregon State University (OSU) model [38] have been imposed. ROMS has been initialized with conditions (3-D velocity, depth-integrated2-D velocity, free-surface level, temperature and salinity) from an operational version running at the University of Ancona [39]. Atmospheric forcings (viz. air temperature and pressure, wind speed, air humidity, cloud cover, rain intensity, shortwave solar radiation) for both grids were provided by the high-resolution COSMO-I7 model [22], a mesoscale model developed in the framework of the COSMO Consortium (www.cosmo-model.org). The effect of WCI on wave power has been estimated running COAWST (Table 1) on the two grids 2-way coupled (2WC runs) between SWAN and ROMS, and simulating the waves on the fine grid without the inclusions of circulation effects (UNC run).

3. Wave power assessment

3.1. Observations at “Acqua Alta”

Wave power at oceanographic tower “Acqua Alta” was computed using Eq. (3) which accounts for the water depth in the wave dispersion relation. We have transformed measured T_{m01} to T_e, aware that since $P \propto H_{m0}^2 T_e$ an error in the wave period estimation is less effective than one in the wave height estimation [6]. Hence, we used an empirical law achieved from the comparison of data sets gathered in the northern Adriatic Sea: $T_e = 1.053 T_{m01}$, which is consistent with other authors' estimates [40].

Wave climate at “Acqua Alta” (see Fig. 2 and Table 2) is characterized by an average significant wave height of 0.45 m, with peaks up to 4.78 m. In terms of potential wave power, the average P is equal to 1.5 kW/m, in agreement with the estimates of other authors in the Adriatic Sea: Liberti et al. [11] obtained an average wave power of 3.0 kW/m at most from a 10-year long model simulation (2001–2010). In the Gulf of Venice, Vicinanza et al. [10] calculated a mean value of 1.7 kW/m at “Punta della Maestra” buoy during almost one year measurements (2004). However, wave powers greater than 40 kW/m can occur during intense storms: for example, in autumn 2000 and winter 2002, 94.2 and 81.8 kW/m were observed, respectively (Fig. 2, bottom panel). The total potential energy E_{tot} generated within the observed period is in the order of 150 MW h/m, growing almost linearly in time, locally increasing during winter months.

A wave power average-year (Fig. 3, left panel) shows that the winter days could reach daily wave powers up to almost 6 kW/m. Again, the growth line of the total potential wave energy, 12 MW h/m per year on average, is steeper during the winter months. In this Figure, right panel shows the duration curve as estimated at “Acqua Alta”. The values exceeding 365 and 180 days per year, $P_{365} = 0.2$ kW/m and $P_{180} = 1.1$ kW/m, respectively, point out however that in the northern Adriatic Sea periods of calm are rather frequent.

The total wave energy potentially produced at “Acqua Alta” within each (H_{m0}, T_{m01}) sea state is shown in Fig. 4. The most energetic sea state is characterized by 1.80 m of significant wave height H_{m0} and 4.50 s of mean wave period T_{m01}. Since it represents the 0.7% of the total observed sea states, 3 h each, it generated 6.65 MW h/m over 15 years. Higher wave power sea states were observed, for example $H_{m0} = 4.60$ m and $T_{m01} = 7.00$ s, but with a very low probability of occurrence, thus generating consequently low energy. Fig. 4 shows that the most probable sea state at oceanographic tower “Acqua Alta” was $H_{m0} = 0.20$ m and $T_{m01} = 2.50$ s.

With the aim of discussing the choice of the wave power formula (3), we have investigated the consequences of applying Eq. (7) instead, which holds in deep waters ($d/L > 0.50$) but it is often applied for wave power estimates independently from the relative water depth d/L, especially in the early stages of the assessment process. The comparison is shown in Fig. 5, where the deep water formula (power P_{dw}) is plotted against the general equation of P. Within the analyzed period, the minimum observed d/L_m was equal to 0.17, and 15% of observed sea states had $d/L_m < 0.50$ (being L_m the mean wavelength). A trend of underestimation of wave power, pointed out by the slope of the best fit-line ($p = 0.87$), is observed using the deep waters formula. As expected, the higher the waves (and thus the wave power), the higher the underestimation. For example, the most energetic sea states in Fig. 4, such that $H_{m0} = 1.80$ m and $T_{m01} = 4.50$ s, reaches 7.6 kW/m, which is reduced

Table 1
COAWST setups used to simulate waves and currents in the Adriatic Sea (coarse grid, C) and Gulf of Venice (fine grid, F).

Run name	Grid resolution	Simulated period	WCI
$2WC_C$	2.0 km (coarse)	01.09.2010–31.08.2011	2-Way coupling
$2WC_F$	0.5 km (fine)	01.01.2011–31.03.2011	2-Way coupling
UNC_F	0.5 km (fine)	01.01.2011–31.03.2011	Uncoupled

Table 2
Wave measurements at oceanographic tower “Acqua Alta” (1996–2011): significant wave height H_{m0}, mean wave period T_{m01} and calculated wave power P.

Data	Mean	Max	Std
H_{m0} (m)	0.45	4.78	0.51
T_{m01} (s)	3.65	11.90	1.20
P (kW/m)	1.5	94.2	3.3

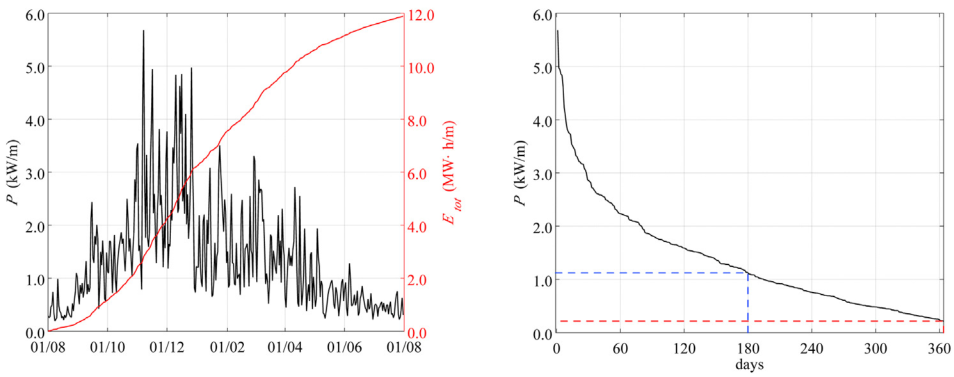

Fig. 3. Wave measurements at oceanographic tower "Acqua Alta". Left panel: wave power P average-year (black) and total potentially produced energy E_{tot} during the average-year (red). Right panel: wave power P duration curve (red line is the power value exceeding 365 days/year, and the blue line is power value exceeding 180 days/year). The average-year starts in August to frame the more significant period, winter, as done for instance in hydrological analyses. (For interpretation of the references to color in this figure legend, the reader is referred to the web version of this article.)

to 7.0 kW/m assuming the deep waters approximation. This underestimation grows up to 20% when considering the highest power sea state observed ($H_{m0} = 4.60$ m and $T_{m01} = 7.00$ s). This error may be falling within the same order of magnitude of those generated by other uncertainties (e.g. quality of input data, space and time variability, etc.). However, standing that a calculation at the actual depth is computationally inexpensive but more accurate, its use is recommended even in the early stages of an assessment process and not only in relatively shallow basins, such as the Adriatic Sea.

3.2. Numerical model outputs

Numerical model runs have been used to estimate the energy resource in each computational cell of the Adriatic Sea. Preliminary, wind inputs at the standard 10-m reference level (V_{10}), computed H_{m0} and T_e have been compared against observations gathered at the oceanographic tower "Acqua Alta" and remotely sensed by altimeters on-board "Jason-1" (NASA–CNES), "Jason-2" (NASA–CNES–EUMETSAT–NOAA) and "Envisat" (ESA) satellites (Fig. 6). The statistical parameters used to compare modeled and observed data are Bias, root-mean-square difference (RMSD), linear correlation coefficient (CC), standard deviation of the fields (R_{std} is the ratio of the modeled to observed standard deviations) [41], and the slope p of the best fit-line between modeled and observed data.

As shown in Table 3, a high-resolution atmosphere model allowed to simulate the wind fields with a high level of accuracy even in a complex area as the northern Adriatic Sea: as a matter of fact, the slope p and the CC values indicate an improvement with respect to a previous analysis carried out on the same region [18].

Simulated waves (Table 4) are less scattered than forcing winds, resulting in an increased significant wave height CC, in the order of 0.90 for all runs, whereas for T_e the cross-correlation is of the same order as wind's one. Same behavior is observed on the slope p. Bias is small for both wave heights and periods, although wave periods reveal a small positive Bias. Standard deviations of modeled and observed wave parameters differ less than 13%.

COAWST outputs have been used to estimate the wave power P, from Eq. (3), and the total wave energy E_{tot} potentially produced by P, from Eq. (5). Figs. 7 and 9 show the mean (left panels) and

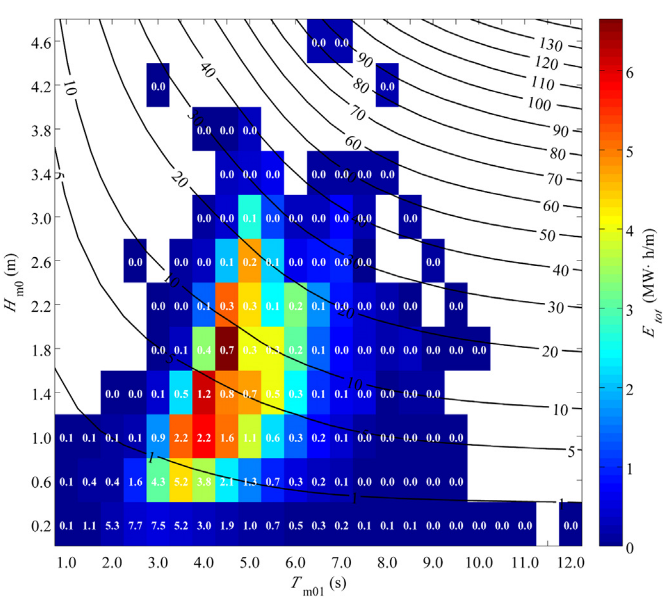

Fig. 4. Total potentially produced wave energy E_{tot} at the oceanographic tower "Acqua Alta", for each measured sea state (H_{m0}, T_{m01}). Black lines are wave power P (kW/m) for each sea state and white numbers are the probabilities of occurrence of each (H_{m0}, T_{m01}) sea state, expressed as percentage.

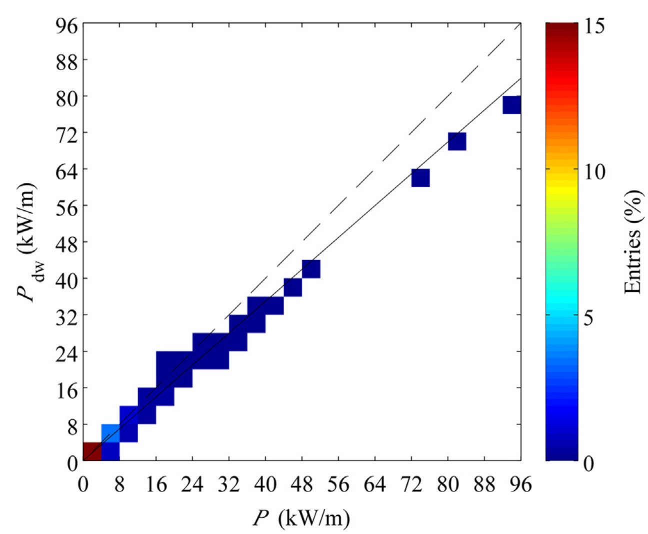

Fig. 5. Scatter diagram of wave power P at "Acqua Alta". P: wave power calculated at the actual "Acqua Alta" tower water depth; P_{dw}: wave power calculated assuming deep waters, according to Eq. (7). Scatter plot has been created by binning the data into 4.0 kW/m bins. The continuous line is the linear regression while the dashed line represents the perfect fit between the two data sets.

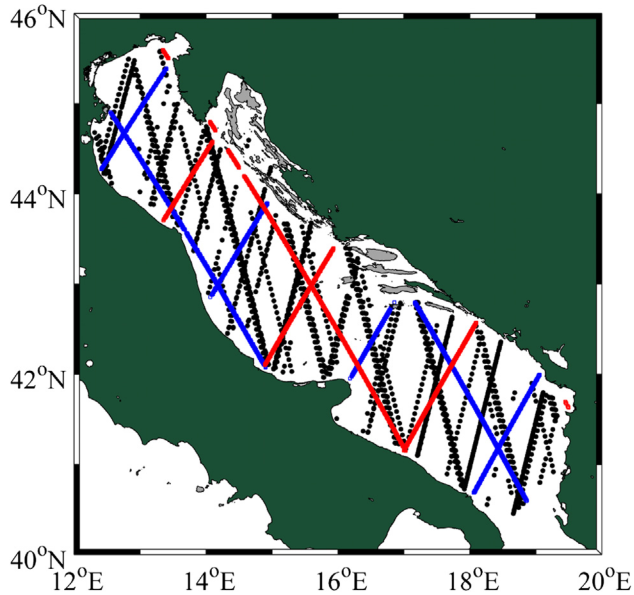

Fig. 6. Sea tracks of satellites "Jason-1" (blue), "Jason-2" (red) and "Envisat" (black) used in COSMO-I7 and COAWST model evaluation. (For interpretation of the references to color in this figure legend, the reader is referred to the web version of this article.)

maximum (right panels) wave power during the simulated intervals, for the three COAWST setups, i.e. $2WC_F$, UNC_F and $2WC_C$, respectively (note that maximum wave powers are the ones occurred at each grid cell during the simulated period and therefore they are not simultaneous.). The correspondent total potentially produced wave energies are shown in Figs. 8 and 10. The role of the most frequent winds on wave energy production is highlighted in Figs. 8 and 10 by distinguishing the contribution of Bora (conventionally selected as the 1st quadrant winds) and Sirocco (conventionally selected as the 2nd quadrant winds). Wave-averaged currents are shown in Fig. 11: the typical ocean circulation pattern during a Bora event is presented on the left panel, and the average during winter months on the right one. Strong Bora winds set up in two gyres with speeds up to 0.50 m/s (left panel), whereas smaller values (in the order of 0.10–0.20 m/s) are typical of the general winter Adriatic Sea circulation.

Differences between the coupled ($2WC_F$) and the uncoupled (UNC_F) runs reveal that in the Gulf of Venice the local effect of currents is able to modify the wave power and the wave energy, in Bora and Sirocco wind conditions. Left panels of Fig. 7 highlight the most productive areas, i.e. the ones experiencing the highest average wave power, while right panels show the highest potential areas, i.e. the ones with the highest maximum wave power. The triangle framed by the southern cape of Istria (Lat = 44° 46′ 05″ N, Lon = 13° 55′ 21″ E), the river Po delta (Lat = 44° 57′ 01″ N, Lon = 12° 25′ 03″ E) and Ancona (Lat = 43° 35′ 57″ N, Lon = 13° 30′ 39″ E), presents one of the highest average potential in the whole Adriatic Sea (see left panel of Fig. 9). This is due to the frequent occurrence of Bora winds during the 2011 winter season and its typical local wave pattern: blowing from the north-eastern quadrant through the Kvarner Gulf, it generates high waves that propagate towards the Italian coasts, despite a relatively short fetch. The same evidence is found in the central panels of Fig. 8, where the contribution of Bora winds has been separated from the total wave energy. However, the peaks of wave power over the northern Adriatic Sea (right panels of Figs. 7 and 9), were generated by both Bora and Sirocco, that has a much longer available fetch than Bora. Results shown in Fig. 10 confirm that Bora contribution is maximum along the northern Adriatic Italian coasts, while Sirocco contribution is maximum over the Dalmatian coasts.

Table 3
Validation statistics for COSMO-I7 modeled wind speed V_{10}: comparisons with observations at oceanographic tower "Acqua Alta" (AA) and remotely sensed (Sat). p: slope of the best fit-line; RMSD: root mean square difference; CC: correlation coefficient; R_{std}: ratio of the standard deviations.

Data	p	Bias	RMSD	CC	R_{std}
V_{10}-AA	0.90	−0.18 m/s	2.12 m/s	0.77	1.03
V_{10}-Sat	0.99	0.07 m/s	1.82 m/s	0.72	1.11

Table 4
Validation statistics for modeled H_{m0} and T_e: comparisons with observations at oceanographic tower "Acqua Alta" (AA). COAWST runs specifications are summarized in Table 1. p: slope of the best fit-line; RMSD: root mean square difference; CC: correlation coefficient; R_{std}: ratio of the standard deviations.

Run	Data	p	Bias	RMSD	CC	R_{std}
$2WC_F$	H_{m0}	0.98	0.01 m	0.25 m	0.91	1.07
	T_e	0.70	0.61 s	0.98 s	0.69	1.01
$2WC_C$	H_{m0}	0.93	−0.02 m	0.24 m	0.86	1.08
	T_e	0.65	0.36 s	0.87 s	0.67	0.96
UNC_F	H_{m0}	1.02	0.01 m	0.27 m	0.91	1.13
	T_e	0.73	0.58 s	1.01 s	0.68	1.06

To quantify the WCI effect on wave power, wave parameters were extracted from model runs $2WC_F$ and UNC_F at the computational cells nearest to the expected "Acqua Alta" tower position. The time series of observed and modeled wave power P during the 3 winter months of 2011 are shown in Fig. 12, where it can be noted that the main effect of WCI is to reduce the wave power, as a consequence of the wave flattening. The comparison statistics of modeled and observed wave power is given in Table 5. The slope p of the best fitting line approaches the unity when the current effect is accounted by the wave model ($2WC_F$ run), whereas an overestimation of wave power is provided by SWAN when the model was run uncoupled (UNC_F run). Bias and RMSD are smaller for the coupled run, while there is a small difference of CC between coupled and uncoupled run, revealing that ocean current leave unchanged the wave storms shape. Also note that the standard deviation of $2WC_F$ results is closer to the observed value.

The consequence of coupling wave and ocean models has been evaluated in the Gulf of Venice, by comparing the model results between UNC_F and $2WC_F$ runs. Fig. 13 shows the percentage differences Δ of the average wave power P and of the potentially produced wave energy E_{tot}, expressed as:

$$\Delta\langle P\rangle = \frac{\langle P\rangle_{UNC} - \langle P\rangle_{2WC}}{\langle P\rangle_{2WC}} \cdot 100 \tag{8}$$

$$\Delta E_{tot} = \frac{E_{tot,UNC} - E_{tot,2WC}}{E_{tot,2WC}} \cdot 100 \tag{9}$$

Fig. 13 highlights that both wave power and energy are generally overestimated if current effect is not accounted in the wave modeling. A maximum overestimation of approximately 30% has been found on the west Adriatic coast, since Bora winds prevailed during the three simulated winter months. In fact, as long as the surface hydrodynamics of a shallow semi-enclosed basin is mainly driven by wind, waves and current propagate along the same direction, especially during Bora storms [17] (Fig. 11). The effect on waves in a moving medium can be easily described for a single component of the energy spectrum in

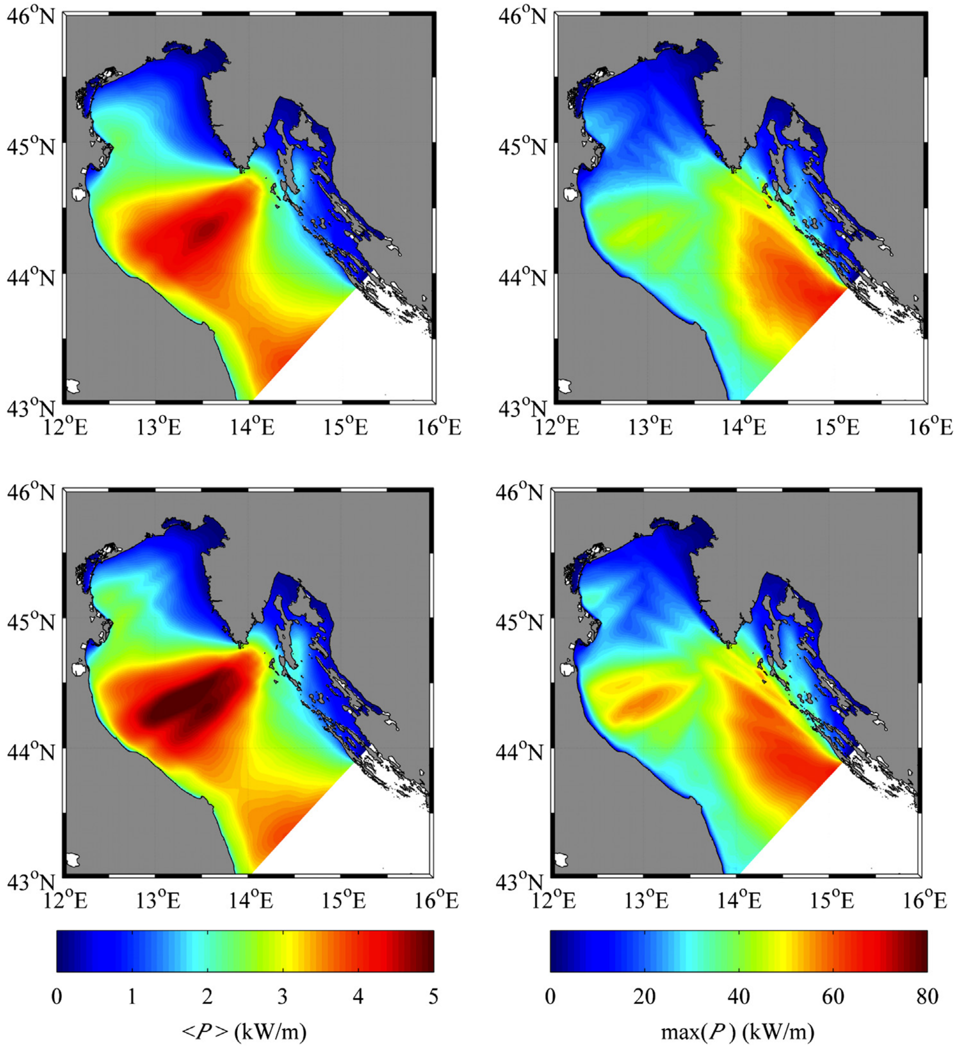

Fig. 7. Average (left panels) and maximum (right panels) wave power over the northern Adriatic Sea. $2WC_F$ (top panels) and UNC_F (bottom panels) runs.

absence of breaking. In this case, the local wave amplitude reads as [42]

$$\frac{A}{A_0} = \frac{c_{g,0}}{\sqrt{c_g(c_g + 2U)}} \tag{10}$$

where A is the wave amplitude and c_g is the wave group speed in presence of an ambient current U, (variables in a still medium are marked by the subscript 0). Hence, in accordance to the wave action balance [43,44], wave heights are modified by the ocean currents, experiencing an increase/decrease of energy when the waves propagated in an opposite/following ambient current. Consequently, during Bora storms, a flattening of waves, i.e. a reduction in wave height and steepness, produces a reduction of P and E_{tot}, which are proportional to H_{m0}^2. The flattening effect is much higher for Bora-generated waves than Sirocco ones, because in the northern Adriatic Sea the latters' direction of propagation is not the same as that of surface currents. As a consequence, accounting for WCI, the observed reduction of wave power magnitudes is much higher in the triangular Bora pattern than along the Dalmatian coasts, where Sirocco winds dominate. A further evidence of this behavior can be found comparing top-left panel of Fig. 7 with bottom-left panel of the same Figure or top-left panel of Fig. 8 with its bottom-left panel.

4. Final considerations

This study has presented a coupled wave-ocean numerical approach to improve the evaluation strategy of the potential wave power that can be extracted at a given sea site. Results obtained, together with a 15 year-long wave time series at "Acqua Alta" oceanographic tower, allowed us to characterize the energy resource in the northern Adriatic Sea where, to our best knowledge, accurate and long-term estimates have not been performed until now.

Northern Adriatic Sea characterization obtained from "Acqua Alta" observations over the 15 years (August, 1996–July, 2011) confirmed that it is a low average wave power area (1.5 kW/m). Although this is in agreement with previous estimates in the basin [10,11], we found that wave power may reach considerable values, up to 94.2 kW/m, comparable with those encountered in the more productive regions of the world. Besides this, the frequent periods of calm observed may be optimal for safe installation and maintenance of the WECs, suggesting the northern Adriatic Sea and the Gulf of Venice as good testing sites for these devices. On the same data set we have also found that an underestimation on wave power (13% on average, 20% at most) would have occurred, should a deep waters formula had been applied independently from the relative water depth, concluding that Eq. (3) should then be routinely employed.

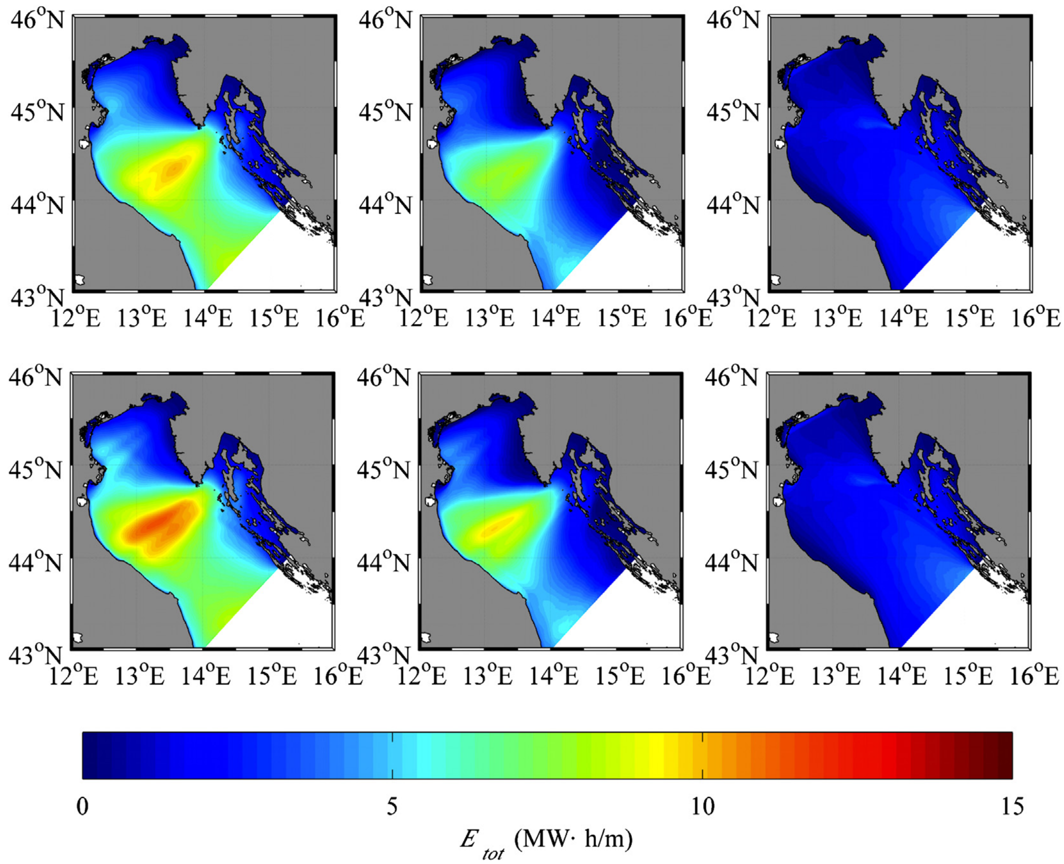

Fig. 8. Total potentially produced wave energy E_{tot} over the northern Adriatic Sea. All winds contribution (left panels), Bora winds contribution (central panels), Sirocco winds contribution (right panels). $2WC_F$ (top panels) and UNC_F (bottom panels) runs.

In this study, the numerical model runs performed enabled us to investigate and for the first time quantify the effect of WCI inclusion in the numerical modeling for wave energy assessment. Results obtained from observations at "Acqua Alta" tower were taken as the benchmark. With respect to them, a small underestimation (1%) of the wave power was observed when including ($2WC_F$ run) WCI modeling, while a much larger value (12%) was observed when neglecting them (UNC_F run). Then, assuming 2 way-coupled run results as the reference, we compared the northern Adriatic Sea wave power fields. A more accurate assessment was performed

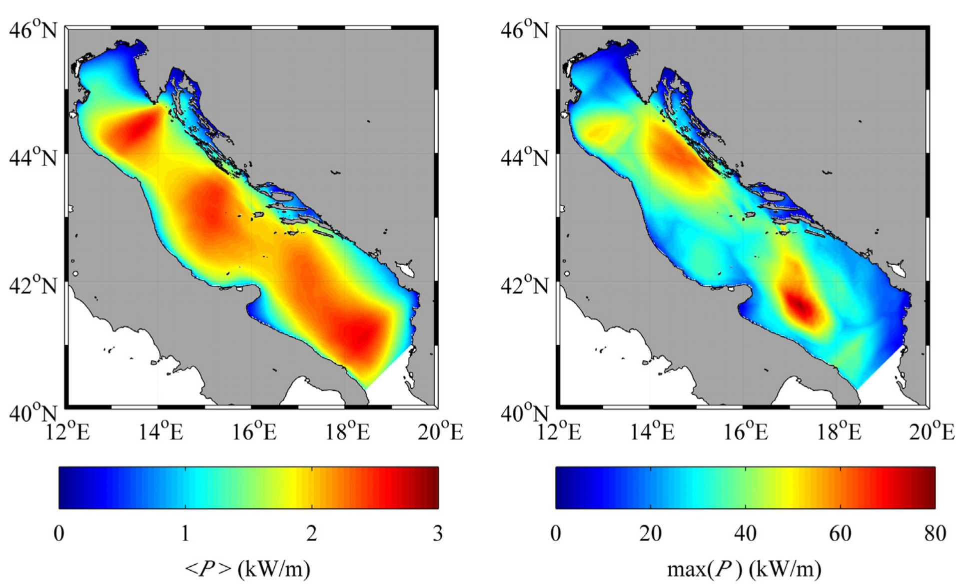

Fig. 9. Average (left panel) and maximum (right panel) wave power over the whole Adriatic Sea. $2WC_C$ run.

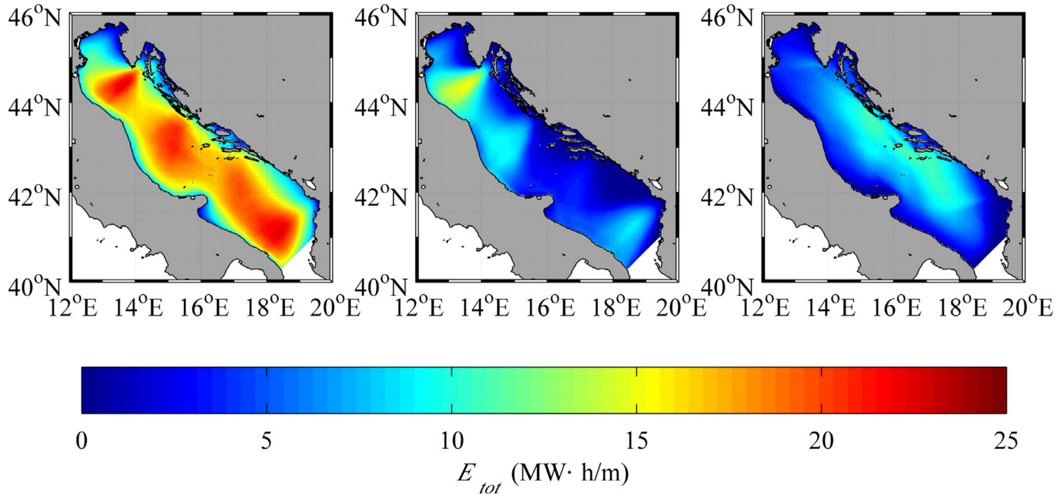

Fig. 10. Total potentially produced wave energy E_{tot} over the whole Adriatic Sea. All winds contribution (left panel), Bora winds contribution (central panel), Sirocco winds contribution (right panel). $2WC_C$ run.

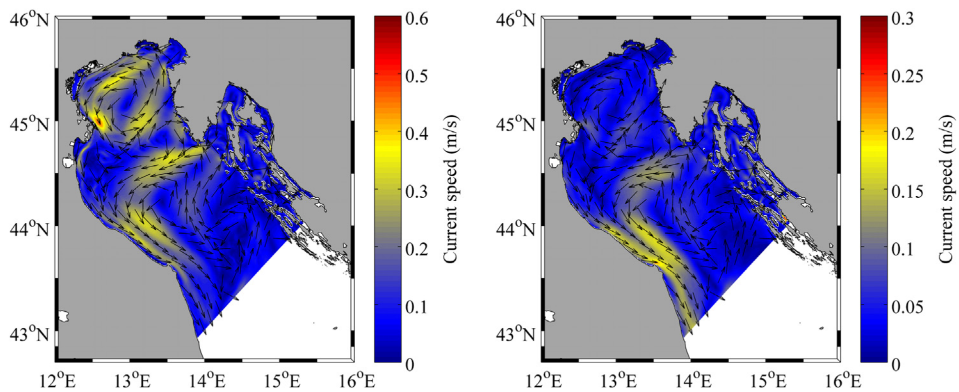

Fig. 11. Modeled wave-averaged currents (m/s) over the northern Adriatic Sea. Black arrows show local currents direction. Left panel: Bora event (January 27–29th, 2011); right panel: average value over the three simulated winter months (January–March, 2011). 2WCF run.

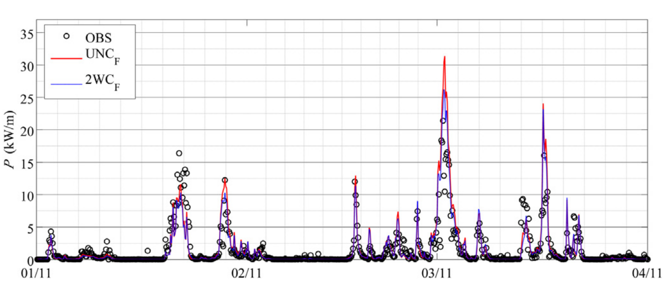

Fig. 12. Time series comparison of modeled (UNC_F and $2WC_F$) and observed (OBS) wave power P at the oceanographic tower “Acqua Alta”.

Table 5
Statistics of modeled wave power P at oceanographic tower “Acqua Alta”, compared with observed wave power, for the winter period January–March, 2011. p: slope of the best fit-line; RMSD: root mean square difference; CC: correlation coefficient; R_{std}: ratio of the standard deviations.

Run	p	Bias	RMSD	CC	R_{std}
$2WC_F$	0.99	0.0 kW/m	1.8 kW/m	0.86	1.15
UNC_F	1.12	−0.2 kW/m	2.1 kW/m	0.85	1.31

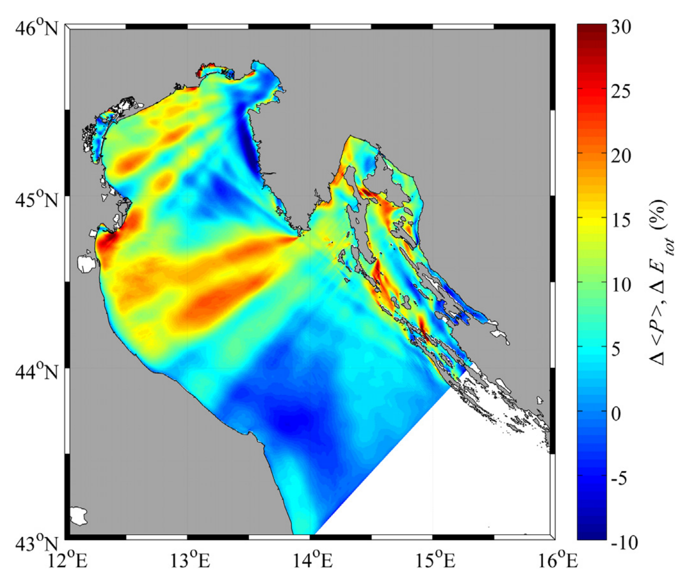

Fig. 13. Comparison between uncoupled (UNC_F) and 2 way-coupled ($2WC_F$) COAWST runs. $\Delta\langle P\rangle$: percentage difference of mean wave power $\langle P\rangle$, Eq. (8); ΔE_{tot}: percentage difference of total potentially produced energy E_{tot}, Eq. (9).

taking into account the WCI, otherwise wave power and total potentially produced energy would have been overestimated up to the 30% on mean value.

This work confirmed that the Adriatic Sea is not eligible for being an optimal wave energy production site, especially when compared to other sites within the Mediterranean region [11] or the oceans [8], but allowed to forward a methodology to improve the assessment of wave power, in particular where currents are not negligible compared to wave group celerity. In any case, should this assessment reveal significant potential production levels, it has to be supported by further studies accounting for the seasonality and climate variability.

Acknowledgments

The work was supported by the FIRBRBFR08D825_001 grant (Project "DECALOGO"). The authors gratefully acknowledge the partial support from the ECFP7/2007-2013 under grant agreement no 242284 (Project "FIELD_AC"). ARPA-EMR is thanked for providing COSMO-I7 meteorological forcings and Luigi "Gigi" Cavaleri for collecting and organizing "Acqua Alta" tower and satellite data.

References

[1] Jeffrey H, Sedgwick J. ORECCA European offshore renewable energy roadmap. URL, www.orecca.eu; 2011.
[2] Marine renewable integrated application platform, deliverable D1.5. URL, www.marina-platform.info; 2013.
[3] Ingram D, Smith G, Bittencourt-Ferreira C, Smith H. Protocols for the equitable assessment of marine energy converters. URL, www.equimar.org; 2011.
[4] Gunn K, Stock-Williams C. Quantifying the global wave power resource. Renewable Energy 2012;44:296–304.
[5] Falcão A. Wave energy utilization: a review of the technologies. Renewable and Sustainable Energy Reviews 2010;14(3):899–918.
[6] Cornett A. A global wave energy resource assessment. In: Proceedings of the 18th international offshore and polar engineering conference, Vancouver, Canada 2008;vol. 1. p. 1–9.
[7] Pontes M, Aguiar R, Pires H. A nearshore wave energy atlas for Portugal. Journal of Offshore Mechanics and Arctic Engineering 2005;127:249–55.
[8] Barstow S, Mørk G, Lønseth L, Mathisen J. Worldwaves wave energy resource assessments from the deep ocean to the coast. In: 8th European wave and tidal energy conference, Uppsala, Sweden 2009. p. 149–59.
[9] Pontes T, de Bettencourt L, Athanassoulis G, Tsoulos I, Nakos B, Skarsoulis E, et al. WERAtlas, European wave energy atlas. Tech. Rep.; Technical Report, European Commission JOULE programme, contract number JOU2-CT93-0390 1997.
[10] Vicinanza D, Cappietti L, Ferrante V, Contestabile P. Estimation of the wave energy in the Italian offshore. Journal of Coastal Research 2011;64:613–7.
[11] Liberti L, Carillo A, Sannino G. Wave energy resource assessment in the Mediterranean, the Italian perspective. Renewable Energy 2013;50(0):938–49. http://dx.doi.org/10.1016/j.renene.2012.08.023.
[12] Cruz J. Ocean wave energy: current status and future prespectives. Green Energy and Technology; Springer; 2008.
[13] Vicinanza D, Contestabile P, Ferrante V. Wave energy potential in the north-west of Sardinia (Italy). Renewable Energy 2013;50:506–21.
[14] Booij N, Ris R, Holthuijsen L. A third-generation wave model for coastal regions. I: model description and validation. Journal of Geophysical Research Oceans 1999;104(C4):7649–66.
[15] Shchepetkin A, McWilliams J. The regional oceanic modeling system (ROMS): a split-explicit, free-surface, topography-following-coordinate oceanic model. Ocean Modelling 2005;9(4):347–404.
[16] Warner J, Sherwood C, Signell R, Harris C, Arango H. Development of a three-dimensional, regional, coupled wave, current, and sediment-transport model. Computers & Geosciences 2008;34(10):1284–306.
[17] Benetazzo A, Carniel S, Sclavo M, Bergamasco A. Wave-current interaction: effect on the wave field in a semi-enclosed basin. Ocean Modelling 2013. http://dx.doi.org/10.1016/j.ocemod.2012.12.009.
[18] Signell R, Carniel S, Cavaleri L, Chiggiato J, Doyle J, Pullen J, et al. Assessment of wind quality for oceanographic modelling in semi-enclosed basins. Journal of Marine Systems 2005;53(1):217–33.
[19] Bergamasco A, Gacic M. Baroclinic response of the Adriatic Sea to an episode of Bora wind. Journal of Physical Oceanography 1996;26(7):1354–69.
[20] Beg Paklar G, Isakov V, Koracin D, Kourafalou V, Orlic M. A case study of bora-driven flow and density changes on the Adriatic Shelf (January 1987). Continental Shelf Research 2001;21(16–17):1751–83.
[21] Pullen J, Doyle J, Hodur R, Ogston A, Book J, Perkins H, et al. Coupled ocean-atmosphere nested modeling of the Adriatic Sea during winter and spring 2001. Journal of Geophysical Research Oceans 2003;108(C10). 3320–20p.
[22] Steppeler J, Doms G, Schättler U, Bitzer H, Gassmann A, Damrath U, et al. Meso-gamma scale forecasts using the nonhydrostatic model LM. Meteorology and Atmospheric Physics 2003;82(1):75–96.
[23] Saulnier J, Pontes M. Guidelines for wave energy resource assessment and standard wave climate. In: Proceedings of the international conference on ocean energy OTTI, Bremerhaven, Germany 2006.
[24] Ochi M. Ocean waves: the stochastic approach. Cambridge ocean technology series. Cambridge University Press; 2005.
[25] Izadparast AH, Niedzwecki JM. Estimating the potential of ocean wave power resources. Ocean Engineering 2011;38:177–85.
[26] Dykes J, Wang D, Book J. An evaluation of a high-resolution operational wave forecasting system in the Adriatic Sea. Journal of Marine Systems 2009;78: 5255–71.
[27] Bignami F, Sciarra R, Carniel S, Santoleri R. Variability of Adriatic Sea coastal turbid waters from SeaWiFS imagery. Journal of Geophysical Research Oceans 2007;112:C03S10.
[28] Boldrin A, Carniel S, Giani M, Marini M, Aubry F, Campanelli A, et al. Effects of bora wind on physical and biogeochemical properties of stratified waters in the northern Adriatic. Journal of Geophysical Research Oceans 2009;114: C08S92.
[29] Book J, Signell R, Perkins H. Measurements of storm and nonstorm circulation in the northern Adriatic: October 2002 through April 2003. Journal of Geophysical Research Oceans 2007;112:C11S92.
[30] Warner J, He R, Zambon J, Armstrong B. Development of a coupled ocean-atmosphere-wave-sediment transport (COAWST) modeling system. Ocean Modelling 2010;35:230–44.
[31] Kirby J, Chen T. Surface waves on vertically sheared flows: approximate dispersion relations. Journal of Geophysical Research Oceans 1989;94(C1): 1013–27.
[32] Kumar N, Voulgaris G, Warner J, Olabarrieta M. Implementation of the vortex force formalism in the coupled ocean-atmosphere-wave-sediment transport (COAWST) modeling system for inner shelf and surf zone applications. Ocean Modelling 2012;47:65–95.
[33] Mellor GL. The depth-dependent current and wave interaction equations: a revision. Journal of Physical Oceanography 2008;38(11):2587–96.
[34] Uchiyama Y, McWilliams JC, Shchepetkin AF. Wave–current interaction in an oceanic circulation model with a vortex-force formalism: application to the surf zone. Ocean Modelling 2010;34(1):16–35.
[35] Komen G, Hasselmann S, Hasselmann K. On the existence of a fully developed wind-sea spectrum. Journal of Physical Oceanography 1984;14(8): 1271–85.
[36] Hasselmann S, Hasselmann K, Allender J, Barnett T. Computations and parameterizations of the nonlinear energy transfer in a gravity-wave spectrum. Part II: parameterizations of the nonlinear energy transfer for application in wave models. Journal of Physical Oceanography 1985;15(11):1378–91.
[37] Pinardi N, Allen I, Demirov E, De Mey P, Korres G, Lascaratos A, et al. The Mediterranean ocean forecasting system: first phase of implementation (1998–2001). Annales Geophysicae 2003;21:3–20.
[38] Egbert GD, Erofeeva SY. Efficient inverse modeling of barotropic ocean tides. Journal of Atmospheric and Oceanic Technology 2002;19(2):183–204.
[39] Russo A, Coluccelli A, Deserti M, Valentini A, Benetazzo A, Carniel S. An operational coupled wave-current forecasting system for the northern Adriatic Sea. In: EGU general assembly conference abstracts 2012;vol. 14. p. 12947.
[40] Alvarez A. Estimation of available wave power in the near shore area around Hanstholm harbour. Master's thesis. Denmark: Civil Engineering Department, Aalborg University; 2010.
[41] Taylor K. Summarizing multiple aspects of model performance in a single diagram. Journal of Geophysical Research Atmospheres 2001;106(D7): 7183–92.
[42] Phillips OM. The dynamics of the upper ocean. Cambridge University Press; 1977.
[43] Bretherton F, Garrett C. Wavetrains in inhomogeneous moving media. Proceedings of the Royal Society of London Series A Mathematical and Physical Sciences 1968;302(1471):529–54.
[44] Mei C, Stiassnie M, Yue D. Theory and applications of ocean surface theory and applications of ocean surface waves. In: Part 1: linear aspects, part 2: nonlinear aspects. Advanced series on ocean engineering Singapore, vol. 23. World Scientific; 2006.